Check for updates

Constitutive activity of the inhibitory G protein pathway mediated by non-visual opsin Opn7b reduces cFos activity in stress and fear circuits and modulates avoidance behavior

Hanna Böke[1], Hannah Schulte[1], Maria Worm[1], Julia Bihorac[2], Brix Mücher[1], Martin Hadamitzky[2], Ida Siveke[1,3], Stefan Herlitze[1]* and Katharina Spoida[1]

[1]Department of General Zoology and Neurobiology, Ruhr-University Bochum, Bochum, Germany, [2]Institute of Medical Psychology and Behavioral Immunobiology, Center for Translational Neuro-Behavioral Sciences (C-TNBS), University Hospital Essen, University of Duisburg-Essen, Essen, Germany, [3]Bridge Institute of Experimental Tumor Therapy, University Hospital Essen, University of Duisburg-Essen, Essen, Germany

Constitutive activity of G protein-coupled receptors (GPCRs) plays an important role in brain function and disease including neurodegenerative and psychiatric disorders. The non-visual opsin Opn7b is a constitutively active $G_{i/o}$ coupled GPCR which has been used to synchronize neuronal networks. Here we show that expression of Opn7b in the bed nucleus of the stria terminalis and the ventral tegmental area, two interconnected brain areas involved in modulating fear and stress responses, reduces the number of cFos positive neurons and modulates avoidance behavior in mice. Thus, by constitutively activating the $G_{i/o}$ pathway Opn7b can be used as a tool to reduce cFos expression and to link cFos-expressing neurons to network- and pathway-specific behavior.

KEYWORDS

VTA (ventral tegmental area), GPCR (G protein coupled receptor), optogenetics, BNST (bed nucleus of the stria terminalis), cFos, constitutive activity of GPCRs, aversive behavior

Introduction

Constitutive activity of G protein-coupled receptors (GPCRs) refers to their ability to activate signaling pathways in the absence of an agonist. This phenomenon has important implications for receptor function, drug discovery, and the understanding of disease mechanisms. Constitutive activity has been observed in many GPCRs across different families and species and plays important physiological roles, such as providing tonic support for basal neuronal activity (Seifert and Wenzel-Seifert, 2002).

The midbrain dopamine system, which is crucial for processing rewards and associated stimuli such as anxiety, fear and stress, is tightly regulated by various GPCRs. Importantly,

these receptors exhibit agonist-independent intrinsic constitutive activity that contributes to their regulation of the ventral tegmental area (VTA) and its projection targets including the bed nucleus of the stria terminalis (BNST) (Meye et al., 2014). By integrating information from various limbic structures, the BNST is a key structure in regulating and shaping motivated and anxiety related behavior (van de Poll et al., 2023). The BNST and VTA have a direct reciprocal connection, with the BNST serving as a major source of neuropeptide and GABAergic inputs to the VTA (Soden et al., 2022).

Among other brain areas various regions and cell types of the BNST and VTA are activated during stress and fear. Activation of neuronal circuits has been correlated with the induction of immediate early gene expression such as cFos (Chung, 2015; Chowdhury and Caroni, 2018). Acute stressors, such as restraint stress, increase cFos expression and neuronal activity in corticotropin-releasing factor (CRF) neurons in the dorsal BNST. This activation is consistent with the role of BNST CRF neurons in driving negative affective behaviors associated with stress (Maita et al., 2022). In addition, various forms of acute and chronic stress increases cFos expression and neuronal activity in different VTA neuron types including GABAergic and dopaminergic neurons (Lowes et al., 2021; Koutlas et al., 2022; Qi et al., 2022; Yu et al., 2022; Yang et al., 2023). This stress-induced activation of VTA neurons appears to play a role in stress-related behavior and may contribute to the development of anxiety-like behaviors (Qi et al., 2022; Mitten et al., 2024). Thus, elevated cFos expression by stress is correlated with increased network activity in the BNST and VTA. Therefore, decreased neuronal activity and following reduced cFos expression within these areas should modulate stress responses.

We recently characterized a non-visual opsin Opn7b from zebrafish in heterologous expression systems and mouse brain. Opn7b is a reverse photoreceptor, that constitutively activates the $G_{i/o}$ pathway in the dark. This constitutive activity of Opn7b can be switched off by blue-green light (Karapinar et al., 2021). Opn7b is not expressed in mammals but in the brain, eye and testis of adult zebrafish (Davies et al., 2015). Activation of $G_{i/o}$ coupled GPCRs such as inhibitory DREADDs (designer receptors exclusively activated by designer drugs) reduces cFos expression (Armbruster et al., 2007; Bruzsik et al., 2021; Tiwari et al., 2022). Thus we tested whether Opn7b without supplying exogenous ligands or drugs, could reduce cFos expression in anxiety- and fear-related circuits, and thereby affect anxiety- and fear-related behavior. Here we demonstrate that viral-mediated expression of Opn7b in the BNST and the VTA reduces cFos expression and modulates odor-induced avoidance and fear responses.

Materials and methods

Subjects

Adult (>8 weeks old) male C57Bl/6 mice (stock No. #000664, Jackson Laboratory) were used in the present study. Mice were group housed, if possible (2-3 mice/cage), with a 12 h light/dark cycle and constant room temperature. Food and water were available *ad libitum*. The procedures were performed during the light phase. All experiments were approved by the

local ethics committee (Bezirksamt Arnsberg) and animal care committee of Nordrhein-Westfalen (LANUV; Landesamt für Umweltschutz, Naturschutz, und Verbraucherschutz Nordrhein-Westfalen, Germany; AZ: 81-02.04.2021.A412). Studies were conducted in accordance with the European Communities Council Directive of 2010 (2010/63/EU) for care of laboratory animals and supervised by the animal welfare commission of the Ruhr-University Bochum.

Stereotaxic surgery

2/1 pseudotyped adeno-associated viruses (AAV) carrying either the opsin parapinopsin or the constitutively active, $G_{i/o}$-coupled optogenetic tool Opn7b were administered by stereotaxic application. Both optogenetic tools are fused to enhanced green fluorescent protein and expressed under control of the CMV promotor. Mice were initially anesthetized using 5% isoflurane (v/v) whereas isoflurane levels were adjusted to 1.5-2.5% (v/v) for the entire surgery. Carprofen (2 mg/kg) and buprenorphine (0.1 mg/kg) were injected subcutaneously for analgesia. For local anesthetic, lidocaine was applied to the scalp. Virus injection was conducted via pressure injection with customized glass pipets (tip diameter 5-10 µm). For injection into the BNSTad and VTA the following stereotactic coordinates were used, related to Bregma: BNSTad AP +0.26 mm, ML +/−0.75 mm, DV −4.2 mm and VTA AP −2.9 mm, ML +/−0.3 to 0.5 mm, DV −4.8 mm. Mice were bilaterally injected with approximately 0.2 µL of the respective virus. The viral construct were expressed for approximately 2 weeks prior to behavioral testing, as this time frame was shown to be sufficient to induce maximal effect on network modulation (Karapinar et al., 2021).

Behavioral testing

The experimental paradigm used was based on a behavioral paradigm established by Bruzsik and colleagues (Bruzsik et al., 2021). Mice were tested in a behavioral paradigm to investigate innate fear responses using a synthetic analog to a fox anogenital product (2-methyl-2-thiazoline; 2MT). Prior to the behavioral experiments, the mice were handled for 2-3 days. Behavioral testing was carried out in an open field arena (50 × 50 × 38 cm) with white light with a light intensity of ∼1,500 lux in the middle. The 2MT [cat. No. L01329.14, Thermo Fisher (Kandel)] was diluted 1:50 and presented on a filter paper placed in a glass petri dish in one corner. The area around the odor source was defined as the "odor zone" (12.5 x 12.5 cm). Testing was repeated on three consecutive days, with a water condition for baseline measurements and habituation, and two different 2MT conditions which were characterized by the amount of 2MT used (according to Bruzsik et al., 2021; low 2MT: 10 µL, high 2MT: 250 µL). At the start of the behavioral test the mice were placed in the corner opposing the odor zone and were left to freely roam and explore the arena for 10 min. Between individuals, the filter paper was removed, and the arena was cleaned with water and 70% EtOH and left to ventilate for 10 min. Four behavioral variables were used to characterize innate fear responses: (1) the locomotor exploratory

activity, measured by the total distance moved in cm, (2) maximum velocity, (3) time spent in the odor zone, based on the center point of the animal, and (4) time spent freezing. Freezing was defined as the absence of all movement except for respiration for a minimum duration of 2 s. Quantification of all behavioral variables, including freezing, was performed using Ethovision XT 15 software (Noldus), which detects immobility based on minimal pixel changes between consecutive video frames. This automated, frame-by-frame analysis provides an objective and reproducible measure of freezing behavior.

Histology and immunohistochemistry

On the third day of behavioral testing, mice were deeply anesthetized and transcardially perfused with ice-cold PBS (1x) followed by 4% paraformaldehyde in PBS (PFA, w/v, pH 7.4, Sigma Aldrich) 90 min after the test. Brains were postfixed in 4% PFA for 2 h and cryoprotected in 30% sucrose (w/v, Fisher Scientific). For subsequent immunohistochemical stainings, brains were cut into 30 μm sections using a cryostat (CM3050 S, Leica). All stainings were performed free floating using a 24-well plate filled with TBS (50 mM Tris-HCl, 150 mM NaCl, pH 7.5). Sections were blocked with 10% normal donkey serum (NDS, Merck Milipore) in 0.3% TBS-Triton X-100 (TBS-T, triton X-100 in TBS) to reduce non-specific antibody binding. BNST sections were incubated with antibody for cFos (rabbit anti cFos, Cat. No. 226 008, Synaptic Systems) to label neuronal activity. VTA sections were incubated with antibody for cFos, and TH (mouse anti TH, MAB318, Merck Millipore) as a marker for dopaminergic neurons in the VTA. Primary antibodies were incubated in a solution of 3% NDS in 0.3% TBS-T, as well as the secondary antibodies. Secondary antibody solution included donkey anti rabbit Cy5 (Code no. 711-175-152, Jackson Immuno Research) for cFos and donkey anti mouse Dylight 550 (SA5-10167, Thermo Fisher Scientific) for TH.

Imaging and analysis

All immunolabeled brain sections were captured using a confocal laser scanning microscope (TCS SP5II, Leica Microsystems) by using 10x/0.3 NA and 20x/0.7 NA objectives. Z-stack images with 10 optical planes were taken. For quantitative analysis, images were processed using ImageJ software (Schneider et al., 2012). The quantification of c-Fos expression was confined to predefined regions of interest (ROIs), which were delineated using the ImageJ "Polygon Selection" tool based on anatomical landmarks. ROIs were defined in reference to the Allen Mouse Brain Atlas to ensure consistency across animals. Within the BNST, cell counting was restricted to the BNSTad subregion, delineated using the lateral ventricle and the anterior commissure. VTA ROIs were defined using tyrosine hydroxylase (TH) immunoreactivity as a marker for dopaminergic neurons. A minimum of eight corresponding ROIs within the BNST and VTA from both hemispheres were analyzed. cFos immunoreactive cells were counted using a semi-automated quantification with the "Thresholding" and "Analyze Particles" functions (Bihorac et al., 2024). c-Fos-positive cells were defined based on a particle

size range of 15–300 pixel^2 and a circularity between 0.1 and 1.0. Auto fluorescent artifacts, which were mistakenly counted as c-Fos immunoreactive cells, were manually excluded from the analysis. Normalization of c-Fos expression was not performed, as expression pattern and viral spread did not show notable variability across animals, based on consistent eGFP expression.

Statistics

Graphs were generated using SigmaPlot 12.5 (Systat Software) and the data were analyzed with IBM SPSS Statistics (Version 29.0) software. Normality (Shapiro-Wilk test) and homogeneity of variance (Levene's test) were tested before each analysis. An unpaired Student's t-test was utilized to calculate statistical significance. As a non-parametric alternative, the Mann-Whitney U-test was employed. Statistical significance was determined using a critical alpha level of 0.05 ($p \leq 0.05$).

Results

To investigate whether the constitutive activation of the $G_{i/o}$ pathway reduces cFos expression in neuronal circuits and if this reduction can be correlated with a change in behavior we expressed Opn7b, a constitutively active and as a control parapinopsin, a non-constitutively active GPCR, in neuronal circuits associated with stress-induced behaviors (Eickelbeck et al., 2019; Karapinar et al., 2021). We used a predator odor-evoked innate fear paradigm to test for threat anticipation and fear modulation under ambiguous threats (Bruzsik et al., 2021). 2-Methyl-2-thiazoline (2MT) is an innate fear inducer. It is a synthetic derivative of compounds found in fox anogenital secretions, which naturally evoke fear responses in prey animals (Apfelbach et al., 2015; Rosen et al., 2015).

We first injected male mice with AAV expressing Opn7b or parapinopsin under the CMV promotor in the BNST. Two weeks post-injection, we conducted behavioral tests comparing control mice, expressing parapinopsin, to those expressing Opn7b (Figure 1A). Animals were exposed to water or to two different dosages of 2MT and various behavioral parameters including total distance moved, mean velocity of movement, time spent in odor zone, and freezing were analyzed (Figures 1B-F). We found that Opn7b expressing mice in comparison to parapinopsin expressing mice revealed a decrease in the total distance moved at high 2MT concentrations (Figure 1C) and a decrease in the time spent in the odor zone at low 2MT concentration (Figure 1E). The decrease in time spent in the odor zone suggests an increase in avoidance behavior when Opn7b is expressed in the BNST (Albrechet-Souza and Gilpin, 2019; Weera et al., 2021). Ninety minutes after the behavioral experiment mice were sacrificed and cFos expression was compared between parapinopsin and Opn7b expressing mice. We found that the number of cFos expressing cells in the BNST was reduced by 33% in Opn7b expressing mice in comparison to parapinopsin expressing mice (Figures 1G,I) with no change in cFos expression in the VTA (Figures 1H,J).

Since the BNST is interconnected with the VTA and both structures contribute to avoidance behavior, we next injected male mice with AAV expressing Opn7b or parapinopsin in the VTA and
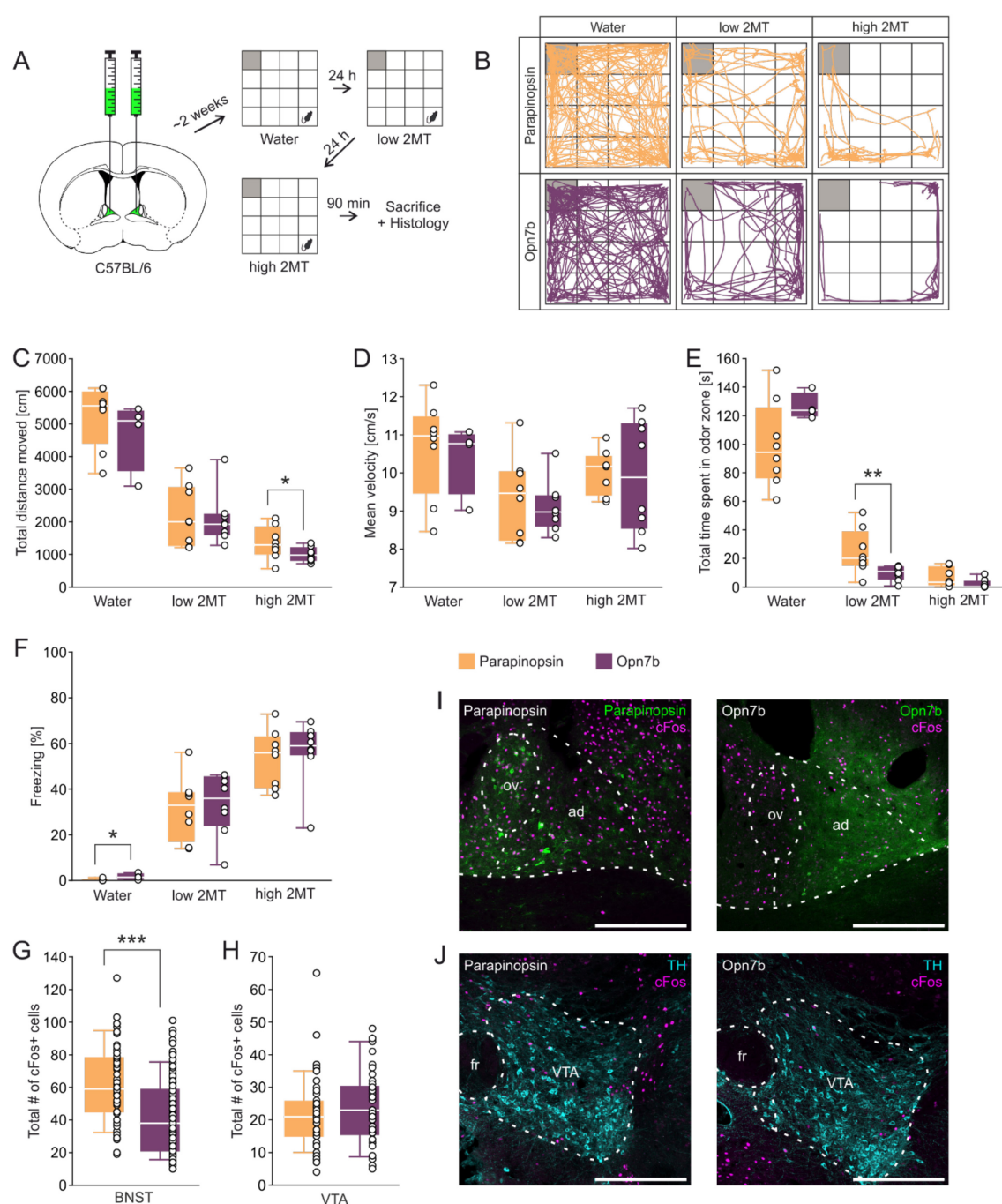
FIGURE 1

Injection of the constitutively active optogenetic tool Opn7b into the BNST reduces cFos expression in the BNSTad. **(A)** Stereotactic injection of the viral constructs encoding either Opn7b or parapinopsin into the anterodorsal nucleus of the bed nucleus of the stria terminalis (BNSTad) of C57BL/6 mice followed by behavioral testing in water and in the 2-methyl-thiazoline (2MT) paradigm with the gray square representing the odor zone. **(B)** Exemplary trajectory plots of individual mice of both groups exposed to water as well as low and high 2MT condition in an open field arena. **(C)** Mice expressing Opn7b in the BNST show a decreased total distance moved compared to mice expressing parapinopsin in the high 2MT condition [$t_{(14)}$ = 1.84, p = 0.044]. **(D)** No differences between groups in the mean velocity in all conditions were found. **(E)** Opn7b injection decreased the time spent in the odor zone only during low 2MT exposure (U = 7.00; z = −2.626, p = 0.007, r = 0.66) but not high 2MT exposure or the water condition. **(F)** Mice expressing Opn7b in the BNST showed less freezing in the water condition (U = 28.00; z = 2.075, p = 0.048, r = 0.60) compared to mice expressing parapinopsin. **(G)** The mice expressing Opn7b (total quantified areas: n = 96 derived from 8 animals) show a decrease in the total number of cFos immunoreactive cells in the BNSTad (U = 1667.50; z = −5.116, p < 0.001, r = 0.40) compared to mice expressing parapinopsin (total quantified areas: n = 66 derived from 6 animals). **(H)** There were no differences in the total number of cFos immunoreactive cells in the ventral tegmental area (VTA) between the groups (Opn7b: total quantified areas: n = 46 derived from 4 animals, parapinopsin: total quantified areas: n = 68 derived from 6 animals). **(I)** Representative images of the injected BNST region showing cFos expression and parapinopsin or Opn7b distribution. ov, oval nucleus of the BNST; ad, anterodorsal nucleus of the BNST. **(J)** Representative images of the VTA region (tyrosine-hydroxylase (TH) used as a marker for dopaminergic neurons) showing cFos expression in mice expressing either parapinopsin or Opn7b in the BNST. fr, fasciculus retroflexus. Scale bar = 300 μm Data are shown as means ± SEM. *p ≤ 0.050, **p ≤ 0.010, ***p ≤ 0.001 (unpaired Student's t-test).
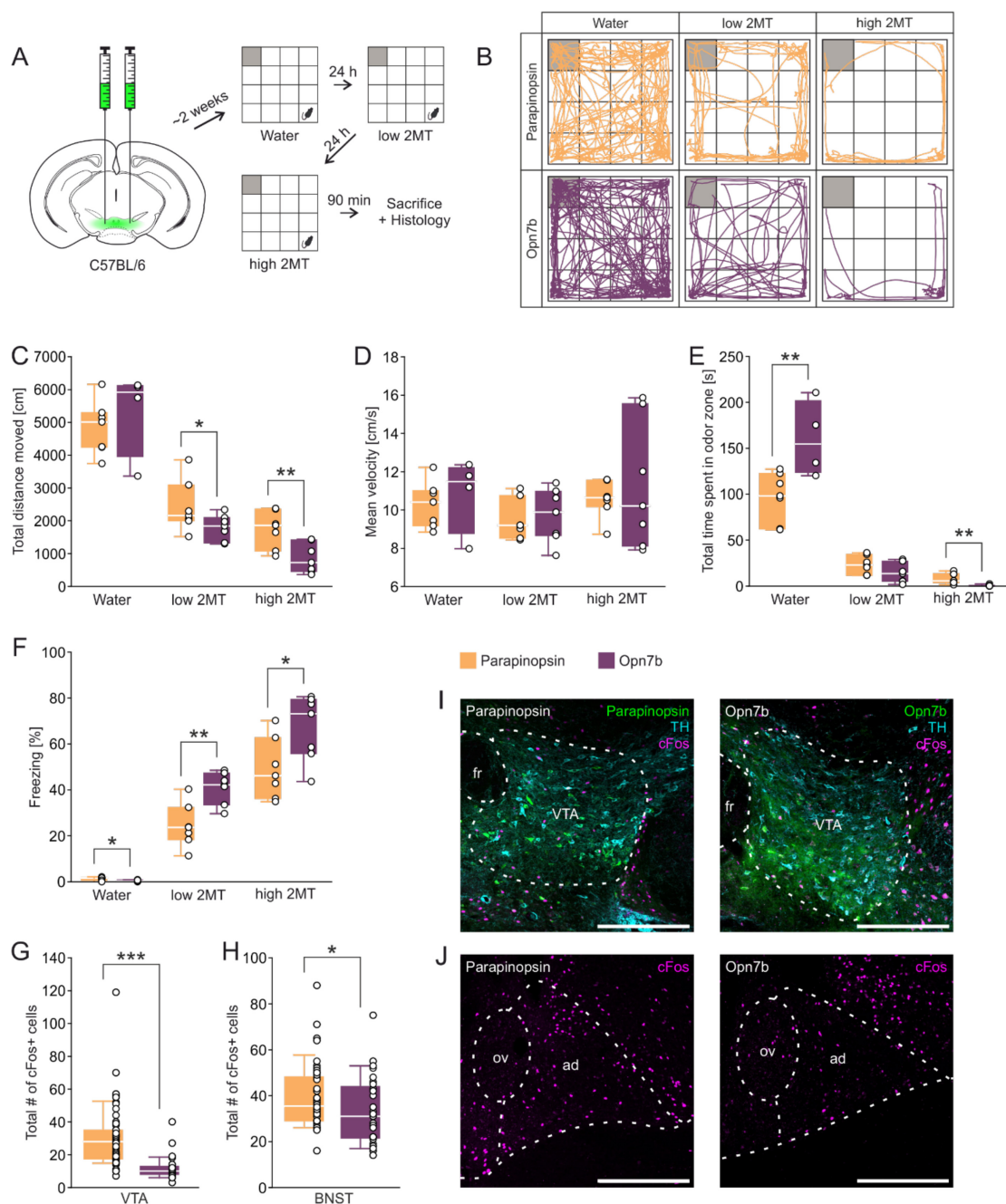
FIGURE 2

Injection of the constitutively active optogenetic tool Opn7b into the VTA reduces cFos expression in the VTA and BNSTad. **(A)** Stereotactic injection of the viral constructs encoding either parapinopsin or Opn7b into the ventral tegmental area (VTA) of C57BL/6 mice followed by behavioral testing in water and in the 2-methyl-thiazoline (2MT) paradigm with the gray square representing the odor zone. **(B)** Exemplary trajectory plots of individual mice of both groups exposed to water as well as low and high 2MT condition in an open field arena. **(C)** Mice expressing Opn7b in the VTA show a decreased total distance moved compared to mice expressing parapinopsin in the low 2MT condition [$t_{(12)}$ = 1.90, p = 0.041] as well as the high 2MT condition [$t_{(12)}$ = 3.20, p = 0.004]. **(D)** No differences between groups in the mean velocity in all conditions were found. **(E)** Opn7b injection increased the time spent in the odor zone during the water condition [$t_{(9)}$ = −3.13, p = 0.006] and decreased it during high 2MT exposure (U = 1.00; z = −3.071, p = 0.001, r = 0.82). **(F)** Mice expressing Opn7b in the VTA showed less freezing in the Water condition [$t_{(9)}$ = 2.15, p = 0.030] but greater freezing percentages when exposed to low [$t_{(12)}$ = −3.72, p = 0.001] and high 2MT compared to mice expressing parapinopsin [$t_{(12)}$ = −2.41, p = 0.016]. **(G)** The mice expressing Opn7b (total quantified areas: n = 33 derived from 3 animals) show a decrease in the total number of cFos immunoreactive cells in the VTA (U = 168.00; z = −6.472, p < 0.001, r = 0.68). (parapinopsin: quantified areas: n = 57 derived from 5 animals). **(H)** Mice expressing Opn7b (total quantified areas: n = 29 derived from 3 animals) in the VTA show a decrease in the total number of cFos immunoreactive cells in the anterodorsal nucleus of the bed nucleus of the stria terminalis (BNSTad) (U = 470.00; z = −2.145, p = 0.032, r = 0.25) compared to mice expressing parapinopsin (total quantified areas: n = 46 derived from 5 animals) in the VTA. **(I)** Representative images of the injected VTA region (tyrosine-hydroxylase (TH) used as a marker for dopaminergic neurons) showing cFos expression and parapinopsin or Opn7b distribution. fr, fasciculus retroflexus. Scale bar = 300 μm. **(J)** Representative images of the BNST region showing cFos expression in control mice and mice expressing parapinopsin or Opn7b in the VTA. ov, oval nucleus of the BNST; ad, anterodorsal nucleus of the BNST. Scale bar = 300 μm. Data are shown as means ± SEM. *p ≤ .050, **p ≤ .010, ***p ≤ .001 (unpaired Student's t-test).

performed the same experiments as described above (Figures 2A-F). Under low 2MT concentrations we found a decrease in the total distance moved (Figure 2C), and an increase in freezing (Figure 2F) in OPN7 injected mice compared to parapinospin injected mice. In addition, under high 2MT concentrations we observed a decrease in the total distance moved (Figure 2C), a decrease in the time spent in the odor zone (Figure 2E), and an increase in freezing in comparison to parapinopsin expressing mice (Figure 2F). In addition, we observed an increase in time spent in the odor zone (Figures 2E) if only water was presented in Opn7b in comparison to parapinopsin expressing mice. The experiments suggest that expression of Opn7b in the VTA increases avoidance related behavior in mice. We next quantified cFos-expressing neurons and found that Opn7b expression in comparison to parapinopsin in the VTA reduced their number by 61% (Figures 2G,I) and by 17% in the BNST (Figures 2H,J).

Discussion

The main goal of this study was to determine whether the constitutive activation of the $G_{i/o}$ pathway by Opn7b suppresses cFos expression in neuronal circuits and if this suppression correlates with behavioral changes. Indeed, in comparison to the non-constitutively active parapinopsin expression of Opn7b in the BNST and the VTA reduced cFos expression and increased odor-induced avoidance and fear behavior. The reduction in cFos expression can be explained by the constitutive activation of the $G_{i/o}$ pathway mediated by Opn7b (Karapinar et al., 2021). Constitutive activity of Opn7b stabilizes the resting membrane potential, while deactivation of Opn7b-mediated constitutive activity synchronizes neuronal network activity (Karapinar et al., 2021). The activation of the $G_{i/o}$ pathways seems to be important to inhibit the activation of the immediate early genes in neurons. A reduction in cFos activity has also been observed when $G_{i/o}$ coupled inhibitory DREADDs have been expressed and activated in the central nervous system (Bruzsik et al., 2021; Tiwari et al., 2022).

Opn7b-mediated reduction of cFos expression in the BNST and VTA increased avoidance and fear-related behaviors, compared to parapinopsin, in response to potential threats. Both brain areas are involved in encoding avoidance behavior and are reciprocally connected. For example, VTA dopaminergic neurons project into the dorsomedial nucleus of the BNST (Lebow and Chen, 2016), while peptidergic and GABAergic neurons innervate in particular dopaminergic neurons in the VTA (Soden et al., 2022). Thus, it is likely that Opn7b-mediated reduced constitutive baseline activity of GABAergic and dopaminergic projections from the BNST and VTA drives the modulation of innate fear responses. In fact, chemogenetic inhibition of GABAergic neurons in the BNST using $G_{i/o}$-coupled DREADDs increased avoidance behavior and freezing in the presence of cat odors and 2MT (Bruzsik et al., 2021). On the other hand, dopaminergic activity and release in the VTA is increased by cued warning signals leading to avoidance behavior (Duvarci, 2024). We observed, that Opn7b expression in the VTA leads to 61% decrease in cFos positive neurons and a 17% reduction in the BNST. Therefore, constitutively reducing the activity of VTA-dopamine release may silence specific GABAergic populations to increase innate avoidance behavior by disinhibiting stress-promoting circuits. Another possibility is that Opn7b increases the signal-to-noise ratio in the BNST and VTA for incoming threat stimuli leading to strong DA release due to reduced baseline activity of Opn7b-expression cells.

An important question is whether the decreased cFos expression can directly correlate with changes in GPCR-signaling and network activity and avoidance behavior. In our experiments the mean cFos expression in the VTA is negatively correlated with time to freezing (Supplementary Figure 1), which is consistent with the observations that higher DA activity in the medial VTA is negatively correlated with freezing in extinction learning (Cai et al., 2020). A few studies investigated if the inhibition of cFos expression directly alters behavior. For example, inhibiting cFos expression through antisense oligonucleotides in rats resulted in deficits in spatial long-term memory (Gallo et al., 2018). Additionally, various drugs, such as diazepam, or chemogenetic inhibition decreased cFos expression in areas associated with stress, anxiety and avoidance behavior including the BNST (De Medeiros et al., 2005). These experiments suggest that cFos expression can be linked to specific behavioral responses strengthening the possibility of utilizing Opn7b-mediated suppression of cFos for investigating pathway-specific regulation of behavior.

In conclusion, the non-visual opsin Opn7b can be used to increase constitutive $G_{i/o}$ activity in specific brain regions and specific cell-types without supplying exogenous ligands or drugs and is therefore a tool to investigate the role of constitutive GPCR activity in network function and disease.

Data availability statement

The raw data supporting the conclusions of this article will be made available by the authors, without undue reservation.

Ethics statement

The animal study was approved by the local ethics committee (Bezirksamt Arnsberg) and animal care committee of North-Rhine-Westphalia (LANUV). The study was conducted in accordance with the local legislation and institutional requirements.

Author contributions

HB: Conceptualization, Data curation, Investigation, Methodology, Writing – review & editing, Writing – original draft. HS: Conceptualization, Data curation, Investigation, Methodology, Writing – review & editing. MW: Data curation, Formal Analysis, Methodology, Writing – review & editing. JB: Data curation, Investigation, Methodology, Writing – review & editing. BM: Methodology, Writing – review & editing. MH: Conceptualization, Funding acquisition, Resources, Supervision, Writing – review & editing. IS: Conceptualization, Funding acquisition, Resources, Supervision, Validation, Writing – original draft. SH: Conceptualization, Funding acquisition, Resources, Supervision, Validation, Writing –

original draft, Writing – review & editing. KS: Conceptualization, Funding acquisition, Resources, Supervision, Validation, Writing – original draft, Writing – review & editing.

Funding

Acknowledgments

Conflict of interest

The authors declare that the research was conducted in the absence of any commercial or financial relationships that could be construed as a potential conflict of interest.

Generative AI statement

The authors declare that no Generative AI was used in the creation of this manuscript.

Publisher's note

Supplementary material

The Supplementary Material for this article can be found online at: https://www.frontiersin.org/articles/10.3389/fnbeh.2025.1540947/full#supplementary-material

References

Albrechet-Souza, L., and Gilpin, N. W. (2019). The predator odor avoidance model of post-traumatic stress disorder in rats. *Behav. Pharmacol.* 30:105. doi: 10.1097/FBP.0000000000000460

Apfelbach, R., Parsons, M. H., Soini, H. A., and Novotny, M. V. (2015). Are single odorous components of a predator sufficient to elicit defensive behaviors in prey species? *Front. Neurosci.* 9:263. doi: 10.3389/FNINS.2015.00263

Armbruster, B. N., Li, X., Pausch, M. H., Herlitze, S., and Roth, B. L. (2007). Evolving the lock to fit the key to create a family of G protein-coupled receptors potently activated by an inert ligand. *Proc. Natl. Acad. Sci. U. S. A.* 104, 5163–5168. doi: 10.1073/pnas.0700293104

Bihorac, J., Salem, Y., Lückemann, L., Schedlowski, M., Doenlen, R., Engler, H., et al. (2024). Investigations on the ability of the insular cortex to process peripheral immunosuppression. *J. Neuroimmune Pharmacol.* 19:40. doi: 10.1007/S11481-024-10143-9

Bruzsik, B., Biro, L., Sarosdi, K. R., Zelena, D., Sipos, E., Szebik, H., et al. (2021). Neurochemically distinct populations of the bed nucleus of stria terminalis modulate innate fear response to weak threat evoked by predator odor stimuli. *Neurobiol. Stress* 15:100415. doi: 10.1016/J.YNSTR.2021.100415

Cai, L. X., Pizano, K., Gundersen, G. W., Hayes, C. L., Fleming, W. T., Holt, S., et al. (2020). Distinct signals in medial and lateral VTA dopamine neurons modulate fear extinction at different times. *Elife* 9:e54936. doi: 10.7554/ELIFE.54936

Chowdhury, A., and Caroni, P. (2018). Time units for learning involving maintenance of system-wide cFos expression in neuronal assemblies. *Nat. Commun.* 9:4122. doi: 10.1038/s41467-018-06516-3

Chung, L. (2015). A brief introduction to the transduction of neural activity into fos signal. *Dev. Reprod.* 19:61. doi: 10.12717/DR.2015.19.2.061

Davies, W. I. L., Tamai, T. K., Zheng, L., Fu, J. K., Rihel, J., Foster, R. G., et al. (2015). An extended family of novel vertebrate photopigments is widely expressed and displays a diversity of function. *Genome Res.* 25, 1666–1679. doi: 10.1101/gr.189886.115

De Medeiros, M. A., Reis, L. C., and Mello, L. E. (2005). Stress-Induced c-Fos expression is differentially modulated by dexamethasone, diazepam and imipramine. *Neuropsychopharmacology* 30, 1246–1256. doi: 10.1038/sj.npp.1300694

Duvarci, S. (2024). Dopaminergic circuits controlling threat and safety learning. *Trends Neurosci.* 47, 1014–1027. doi: 10.1016/J.TINS.2024.10.001

Eickelbeck, D., Rudack, T., Tennigkeit, S. A., Surdin, T., Karapinar, R., Schwitalla, J. C., et al. (2019). Lamprey parapinopsin ("UVLamP"): A bistable UV-Sensitive optogenetic switch for ultrafast control of GPCR pathways. *ChemBioChem* 21, 612–617. doi: 10.1002/cbic.201900485

Gallo, F. T., Katche, C., Morici, J. F., Medina, J. H., and Weisstaub, N. V. (2018). Immediate early genes, memory and psychiatric disorders: Focus on c-Fos, Egr1 and Arc. *Front. Behav. Neurosci.* 12:79. doi: 10.3389/FNBEH.2018.00079

Karapinar, R., Schwitalla, J. C., Eickelbeck, D., Pakusch, J., Mücher, B., Grömmke, M., et al. (2021). Reverse optogenetics of G protein signaling by zebrafish non-visual opsin Opn7b for synchronization of neuronal networks. *Nat. Commun.* 12:4488. doi: 10.1038/S41467-021-24718-0

Koutlas, I., Linders, L. E., van der Starre, S. E., Wolterink-Donselaar, I. G., Adan, R. A. H., and Meye, F. J. (2022). Characterizing and TRAPing a social stress-activated neuronal ensemble in the ventral tegmental area. *Front. Behav. Neurosci.* 16:936087. doi: 10.3389/FNBEH.2022.936087

Lebow, M. A., and Chen, A. (2016). Overshadowed by the amygdala: The bed nucleus of the stria terminalis emerges as key to psychiatric disorders. *Mol. Psychiatry* 21, 450–463. doi: 10.1038/mp.2016.1

Lowes, D. C., Chamberlin, L. A., Kretsge, L. N., Holt, E. S., Abbas, A. I., Park, A. J., et al. (2021). Ventral tegmental area GABA neurons mediate stress-induced blunted reward-seeking in mice. *Nat. Commun.* 12:3539. doi: 10.1038/s41467-021-23906-2

Maita, I., Roepke, T. A., and Samuels, B. A. (2022). Chronic stress-induced synaptic changes to corticotropin-releasing factor-signaling in the bed nucleus of the stria terminalis. *Front. Behav. Neurosci.* 16:903782. doi: 10.3389/FNBEH.2022.903782

Meye, F. J., Ramakers, G. M. J., and Adan, R. A. H. (2014). The vital role of constitutive GPCR activity in the mesolimbic dopamine system. *Transl. Psychiatry* 4:e361. doi: 10.1038/TP.2013.130

Mitten, E. H., Souders, A., Marron Fernandez, de Velasco, E., and Wickman, K. (2024). Stress-induced anxiety-related behavior in mice is driven by enhanced excitability of ventral tegmental area GABA neurons. *Front. Behav. Neurosci.* 18:1425607. doi: 10.3389/FNBEH.2024.1425607

Qi, G., Zhang, P., Li, T., Li, M., Zhang, Q., He, F., et al. (2022). NAc-VTA circuit underlies emotional stress-induced anxiety-like behavior in the three-chamber vicarious social defeat stress mouse model. *Nat. Commun.* 13:577. doi: 10.1038/s41467-022-28190-2

Rosen, J. B., Asok, A., and Chakraborty, T. (2015). The smell of fear: Innate threat of 2,5-dihydro-2,4,5-trimethylthiazoline, a single molecule component of a predator odor. *Front. Neurosci.* 9:292. doi: 10.3389/FNINS.2015.00292

Schneider, C. A., Rasband, W. S., and Eliceiri, K. W. (2012). NIH Image to ImageJ: 25 years of image analysis. *Nat. Methods* 9, 671–675. doi: 10.1038/NMETH.2089

Seifert, R., and Wenzel-Seifert, K. (2002). Constitutive activity of G-protein-coupled receptors: Cause of disease and common property of wild-type receptors. *Naunyn Schmiedebergs Arch. Pharmacol.* 366, 381–416. doi: 10.1007/s00210-002-0588-0

Soden, M. E., Yee, J. X., Cuevas, B., Rastani, A., Elum, J., and Zweifel, L. S. (2022). Distinct encoding of reward and aversion by peptidergic BNST inputs to the VTA. *Front. Neural Circuits* 16:918839. doi: 10.3389/FNCIR.2022.918839

Tiwari, P., Kapri, D., Vaidya, V. A., Pradhan, A., Balakrishnan, A., and Chaudhari, P. R. (2022). Chronic hM4Di-DREADD-Mediated chemogenetic inhibition of forebrain excitatory neurons in postnatal or juvenile life does not alter adult mood-related behavior. *eNeuro* 9:ENEURO.0381-21.2021. doi: 10.1523/ENEURO.0381-21.2021.

van de Poll, Y., Cras, Y., and Ellender, T. J. (2023). The neurophysiological basis of stress and anxiety - comparing neuronal diversity in the bed nucleus of the stria terminalis (BNST) across species. *Front. Cell. Neurosci.* 17:1225758. doi: 10.3389/FNCEL.2023.1225758

Weera, M. M., Shackett, R. S., Kramer, H. M., Middleton, J. W., and Gilpin, N. W. (2021). Central amygdala projections to lateral hypothalamus mediate avoidance behavior in rats. *J. Neurosci.* 41:61. doi: 10.1523/JNEUROSCI.0236-20.2020

Yang, S. H., Yang, E., Lee, J., Kim, J. Y., Yoo, H., Park, H. S., et al. (2023). Neural mechanism of acute stress regulation by trace aminergic signalling in the lateral habenula in male mice. *Nat. Commun.* 14:2435. doi: 10.1038/S41467-023-38180-7

Yu, X., Zhao, G., Wang, D., Wang, S., Li, R., Li, A., et al. (2022). A specific circuit in the midbrain detects stress and induces restorative sleep. *Science* 377, 63–72. doi: 10.1126/SCIENCE.ABN0853